SHAFT SIGNALS OF SALIENT-POLE SYNCHRONOUS MACHINES FOR ECCENTRICITY AND SHORTED FIELD COIL DETECTIONS

By:

J.S. Hsu
J. Stein

1994 Winter Meeting of the Power Engineering Society, February 1994

IEEE Transactions on Energy Conversion, vol. 9, no. 3, September 1994, pp. 572-578

PR - 188

Center for Electromechanics
The University of Texas at Austin
PRC, Mail Code R7000
Austin, TX 78712
(512) 471-4496

SHAFT SIGNALS OF SALIENT-POLE SYNCHRONOUS MACHINES FOR ECCENTRICITY AND SHORTED-FIELD-COIL DETECTIONS

John S. Hsu (Htsui)

Jan Stein

This paper discusses the relationships between shaft signals and eccentricities of synchronous machines. It also discusses the effects of shorted field coils on the shaft signals. Extensive experimental works conducted on the four and six-pole reluctance machines, and on the wound-field synchronous machine clearly confirm the theoretical predictions.

In order to superpose the shaft signals per revolution the horizontal input of the oscilloscope is changed to a ramp voltage. This sweeping signal is shown in fig. 1. Each cycle corresponds to the time required for one revolution (or two fundamental cycles in this case). Should one decide more fundamental cycles per sweep are needed for clearer loci, the ramp frequency can be changed accordingly. For meaningful traces the ramp sweeping signal should be synchronized with the line frequency.

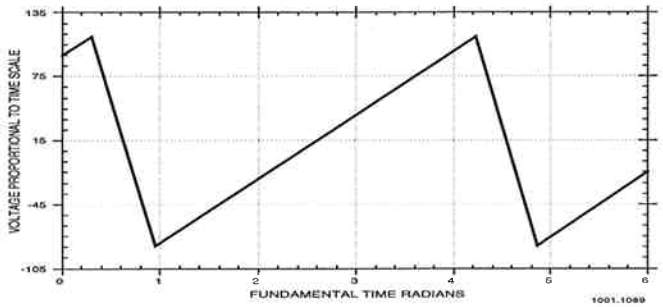

Fig. 1. Synchronized ramp voltage of 30 Hz is used as oscilliscope horizontal input for plotting continuous shaft-flux-linkage loci of 4-pole, 60 Hz synchronous reluctance motors

Fig. 2 shows the superposed loci of continuous shaft-flux-linkage signals for individual revolutions of the synchronous reluctance motors. The thickness of the loci represents the variations that include the effects of the non-synchronized dynamic eccentricities. The overall signal magnitude reflects eccentricities and other relevant asymmetrical situations mentioned previously. The high-magnitude spikes are noises produced by bouncing signal brushes.

The comparison of relative shaft-flux-linkage harmonics at no load between situations with and without a shorted field coil of the same 6-pole wound-field synchronous machine is shown in fig. 3. Two distinctive orders of harmonics around 20 Hz and 160 Hz as predicted are clearly shown in the situation with a shorted field coil (fig. 3b).

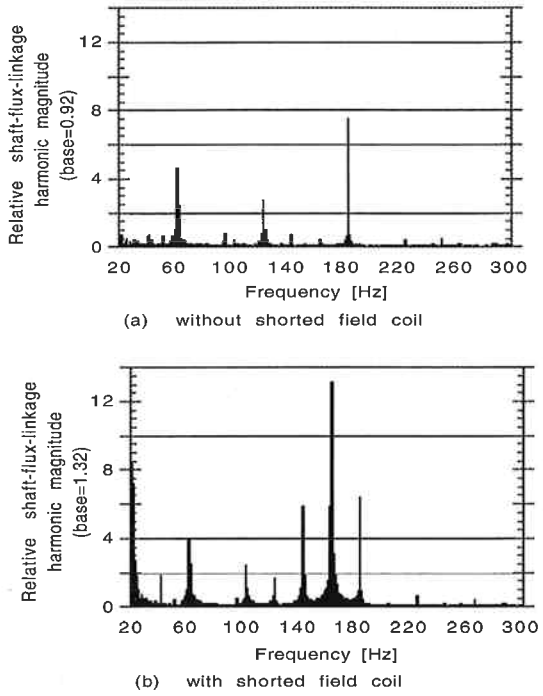

Fig. 3. Comparison of relative shaft-flux-linkage harmonic magnitudes at no load between situations with and without shorted field coil of a 6-pole, synchronous motor excited by pure dc (1.4 and 1.6 amps). Stator line voltage is 230 V at 60 Hz

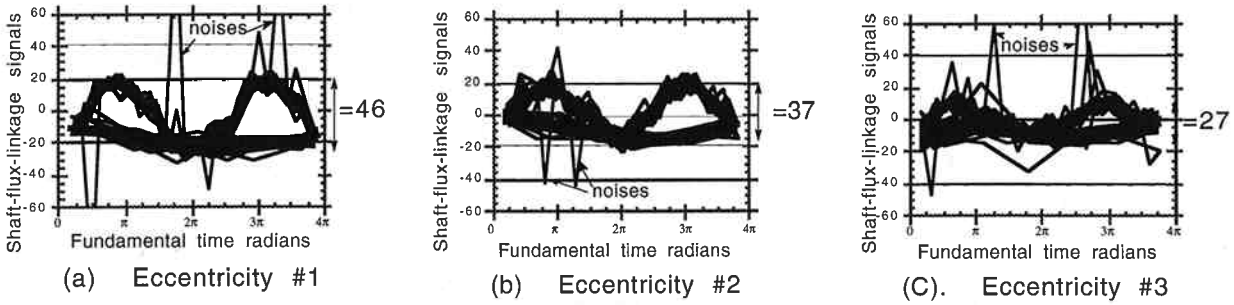

Fig. 2. Significant changes of overall shaft-flux-linkage-signal magnitudes under three different eccentricities of a 4-pole, synchronous reluctance motor. (Loci for continuous shaft-flux-linkage signals of 1.0 second are obtained at 60 Hz, 230 V, and no-load. Eccentricity is only controlled by changing end brackets and fits of bearings. All other parts of the motor remain unchanged)

SHAFT SIGNALS OF SALIENT-POLE SYNCHRONOUS MACHINES FOR ECCENTRICITY AND SHORTED-FIELD-COIL DETECTIONS

John S. Hsu (Htsui)
Senior Member
Center for Electromechanics
The University of Texas at Austin
BRC, Mail Code 77000
Austin, TX 78712

Jan Stein
Member
Electric Power Research Institute
3412 Hillview Avenue
Palo Alto, California 94304

Keywords: Shaft, Voltage, Current, Signal, Loci, Synchronous, Salient, Reluctance, Wound Field, Machine, Steady, Dynamic, Eccentricity

ABSTRACT: Relationships between shaft signals and eccentricities of salient-pole synchronous machines are studied. The magnitude and the thickness of shaft-signal loci reflect steady and dynamic eccentricities. Harmonic components of shaft signals closely relate to shorted field coils. Threshold records can be used for indications of changes in eccentricities and shorted field coils. Extensive experimental work agrees with the theoretical predictions.

I. INTRODUCTION

Shaft voltages and currents have been recognized as bearing failure sources for many years [1]. Various approaches such as grounding brushes for turbogenerators, insulated bearings and (or) insulated couplings for large machines are used to prevent shaft currents going through bearings.

Starting from the last decade or so, the developments of using shaft signals to detect defects in turbogenerators [2-4] have shown possible usage of shaft signals. Meyer, et. al., developed a new grounding design to improve reliability of bearings [3]. Ammann, et. al., discussed the operating experience with RC-grounding device and new possibilities for monitoring conditions of turbogenerators through shaft-to-frame currents in the grounding device [4]. Studies on eccentricities other than using shaft signals can also be traced [6-9]. No sensors mounted in the air gap are required for obtaining shaft signals.

Unlike turbogenerators, most salient-pole electric rotating machines do not use grounding brushes. Although Section 8.16.2.1 of the Hydrogenerator Design Manual [5], issued by the U.S. Department of Interior, calls for a shaft grounding brush mounted below the rotor to provide a continuous ground on the shaft, most old hydrogenerators do not have grounding brushes.

This paper discusses the relationships between shaft signals and eccentricities of synchronous machines. It also discusses the effects of shorted field coils on the shaft signals. Extensive experimental works conducted on the four and six-pole reluctance machines, and on the wound-field synchronous machine clearly confirm the theoretical predictions.

II. GENERATION OF SHAFT VOLTAGES

There are three categories [1] pointed out by Alger et al in the generation of shaft voltages. They are: the alternating current (ac) voltages generated by alternating shaft flux linkages, the homopolar voltages, and the capacitive voltages. This study focuses on the ac voltages generated by shaft flux linkages.

Eccentricity and Shaft Voltage

Fig. 1 shows the shaft-flux linkages of an off-center rotor with respect to air-gap rotating fluxes. A portion of the flux is linked with the shaft. It is clear from this simple model that the greater the eccentricity is, the higher the shaft voltage. If an electric rotating machine viewed from the center of its shaft is perfectly symmetrical, there is no ac shaft voltage generated by alternating shaft flux linkages. A perfectly symmetrical machine means that the flux going on the right-hand side of the center of shaft equals that on the left-hand side. Any possible asymmetrical induced currents in windings or stray paths, variations of magnetic properties, and tolerances in physical dimensions may cause unequal flows of fluxes on the left-hand and the right-hand sides. When this occurs, a circulating flux linked with the shaft is formed. Hence, shaft voltage is generated.

Saturation and Third Harmonic Flux

Conventional synchronous machines are built with ferromagnetic laminations for their magnetic paths. Certain degrees of magnetic saturation are normally encountered for the optimal use of materials. When magnetic saturation occurs, the air-gap flux contains third harmonic flux [10] components. Third-harmonic air-gap flux is a zero sequence flux. Its induced voltages may not show up at the machine terminals. However, since all rotating machines have various degrees of eccentricity, in addition to the fundamental and the non-zero-sequence components, the shaft voltage normally contains a certain third-harmonic voltage.

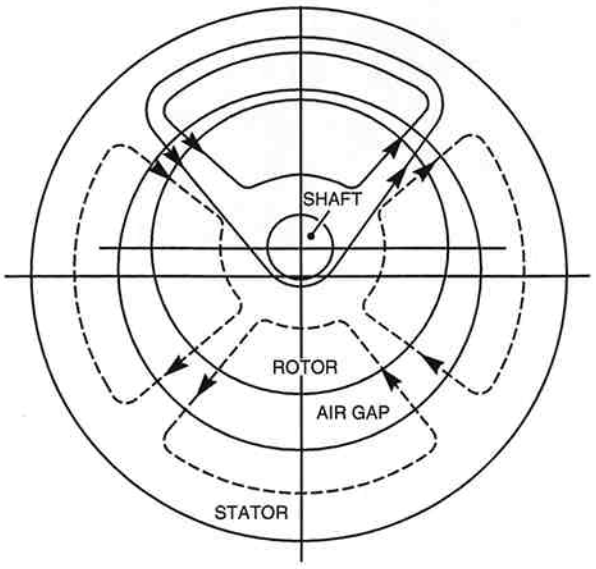

Fig. 1. Shaft flux linkages with respect to air gap rotating fluxes

Salient Poles and Harmonics

Salient poles modify the air-gap flux. For the same air-gap magnetomotive force (MMF), higher flux density is produced along the direct axis than that along the quadrature axis. The permeance of the air gap can be approximately expressed as the sum of a constant component and a $(2 \cdot p)^{th}$ harmonic term rotating at synchronous speed. The symbol p is the number of polepairs.

$$\sin(p \cdot \vartheta - \omega_s \cdot t) \cdot \cos(2 \cdot p \cdot \vartheta - 2 \cdot \omega_s \cdot t) = 0.5 \cdot \begin{bmatrix} \sin(3 \cdot p \cdot \vartheta - 3 \cdot \omega_s \cdot t) \\ -\sin(p \cdot \vartheta - \omega_s \cdot t) \end{bmatrix} \quad (1)$$

where ω_s is the synchronous electric angular velocity.

For a six-pole (i.e., p=3) salient-pole synchronous machine, according to (1) the air gap flux is modulated by the $(2 \cdot p)^{th}$ (i.e., $2 \cdot 3 = 6^{th}$) air-gap permeance harmonic and results in a third and a fundamental flux component.

$$\sin(3 \cdot \vartheta - w_s \cdot t) \cdot \cos(2 \cdot 3 \cdot \vartheta - 2 \cdot w_s \cdot t) = 0.5 \cdot \left[\sin(9 \cdot \vartheta - 3 \cdot w_s \cdot t) - \sin(3 \cdot \vartheta - w_s \cdot t)\right] \quad (2)$$

The third-harmonic flux component rotates at the same speed as the fundamental flux.

Effect of Shorted Field Coils on Shaft Voltages

The shorted turns of field coils can be considered as a normal field coil superimposed with an additional field coil made of the same number of the shorted turns but with opposite flow of current. The cancellation of ampere-turns between the normal and additional field coils simulates the shorted turns. The additional field coil has a two-pole MMF component rotating in synchronization with the rotor. This two-pole component and the main MMF of p polepairs produce (p+1)/2 polepair MMF that is modulated by (p-1)/2 polepairs as follows

$$\sin\left(\vartheta - \frac{\omega_s \cdot t}{p}\right) + \sin(p \cdot \vartheta - \omega_s \cdot t) = 2 \cdot \left\{ \begin{array}{l} \sin\left[\frac{(p+1) \cdot \vartheta}{2} - \left(\frac{p+1}{2 \cdot p}\right) \cdot (\omega_s \cdot t)\right] \\ \cdot \cos\left[\frac{(p-1) \cdot \vartheta}{2} - \left(\frac{p-1}{2 \cdot p}\right) \cdot (\omega_s \cdot t)\right] \end{array} \right\} \quad (3)$$

This (p+1)/2 polepair MMF of (3) is modulated by the $(2 \cdot p)^{th}$ air-gap harmonic permeance component. The resultant air-gap flux has the following components:

$$\begin{aligned} & 2 \cdot \left\{ \begin{array}{l} \sin\left[\frac{p+1) \cdot \vartheta}{2} - \left(\frac{p+1}{2 \cdot p}\right) \cdot (\omega_s \cdot t)\right] \\ \cdot \cos\left[\frac{(p-1) \cdot \vartheta}{2} - \left(\frac{p-1}{2 \cdot p}\right) \cdot (\omega_s \cdot t)\right] \end{array} \right\} \\ & \cdot \cos[2 \cdot p \cdot \vartheta - 2 \cdot \omega_s \cdot t] \\ = & \sin\left[\frac{(1+5 \cdot p) \cdot \vartheta}{2} - \frac{(1+5 \cdot p)}{2 \cdot p} \cdot (\omega_s \cdot t)\right] \\ & \cdot \cos\left[\frac{(p-1) \cdot \vartheta}{2} - \left(\frac{p-1}{2 \cdot p}\right) \cdot (\omega_s \cdot t)\right] \\ & - 0.5 \cdot \sin[p \cdot \vartheta - (\omega_s \cdot t)] \\ & + 0.5 \cdot \sin\left[(1-2 \cdot p) \cdot \vartheta - \frac{(1-2 \cdot p)}{p} \cdot (\omega_s \cdot t)\right] \end{aligned} \quad (4)$$

A major term in (4) is

$$\sin\left[\frac{(1+5 \cdot p) \cdot \vartheta}{2} - \frac{(1+5 \cdot p)}{2 \cdot p} \cdot (\omega_s \cdot t)\right] \cdot \cos\left[\frac{(p-1) \cdot \vartheta}{2} - \left(\frac{p-1}{2 \cdot p}\right) \cdot (\omega_s \cdot t)\right] \quad (5)$$

For example, substituting p=3 of a 6-pole synchronous machine with one shorted field coil into (5) gives the harmonic components of air-gap flux

$$\sin\left[8 \cdot \vartheta - \frac{8}{3} \cdot (\omega_s \cdot t)\right] \cdot \cos\left[\vartheta - \left(\frac{1}{3}\right) \cdot (\omega_s \cdot t)\right] \quad (6)$$

Comparing (6) with the main 6-pole air-gap flux that is equivalent to a 3rd mechanical order of flux on the basis of the mechanical speed (i.e., $\omega_s/3$),

$$\sin(3 \cdot \vartheta - \omega_s \cdot t) \quad or \quad \sin\left[3 \cdot \vartheta - \frac{3}{3} \cdot (\omega_s \cdot t)\right] \quad (7)$$

it is predicted that for the 6-pole machine having a shorted field coil in a pole a distinctive harmonic component around the 8th mechanical order is generated. This 8th mechanical

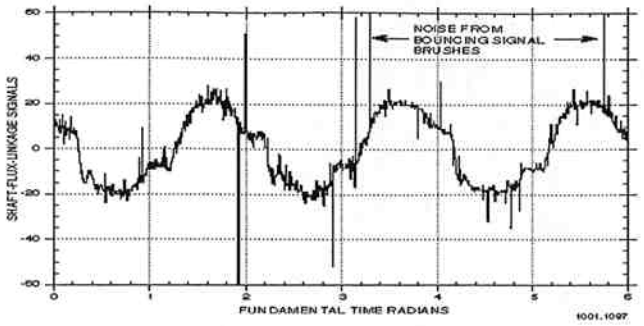

Fig. 3. Shaft-flux-linkage signals of 4-pole #1 synchronous reluctance motor at 60 Hz, 230 V (phase currents: 11.3/10.8/10.8 A.)

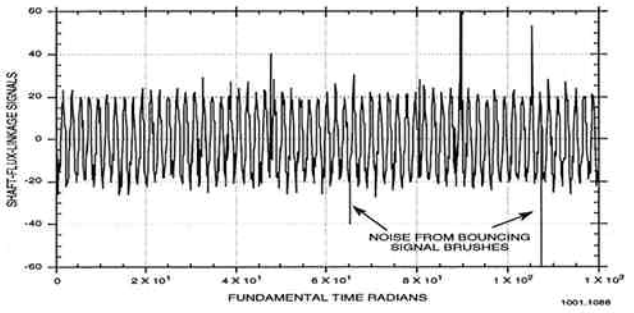

Fig. 4. Shaft-flux-linkage signals of 4-pole #1 synchronous reluctance motor for 1 s at 60 Hz, 230 V (phase currents: 11.3/10.8/10.8 A.)

position may repeat itself every single revolution. Other orders of harmonic fields might not be synchronized with every single revolution. This is the nature of positional characteristic of shaft voltage.

The portion of dynamic eccentricities not in synchronization with every single revolution and the effects of rotating fields other than the fundamental forward field make the shaft-flux-linkage signals not repeating identically every single revolution. Fig. 4 shows the shaft-flux-linkage signals of the same motor of fig. 3 for one second without repeating identically every single revolution (i.e., two fundamental cycles).

In order to superpose the shaft signals per revolution the horizontal input of the oscilloscope is changed to a ramp voltage. This sweeping signal is shown in fig. 5. Each cycle corresponds to the time required for one revolution (or two fundamental cycles in this case). Should one decide more fundamental cycles per sweep are needed for clearer loci, the ramp frequency can be changed accordingly. For meaningful traces the ramp sweeping signal should be synchronized with the line frequency.

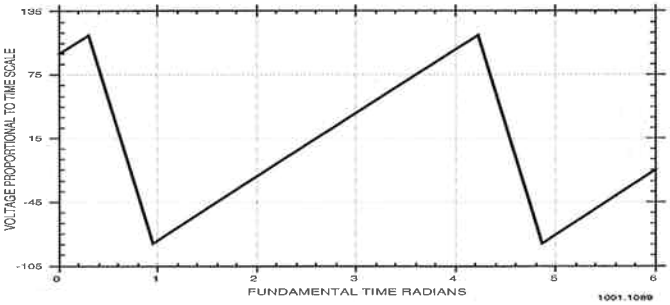

Fig. 5. Synchronized ramp voltage of 30 Hz is used as oscilliscope horizontal input for plotting continuous shaft-flux-linkage loci of 4-pole, 60 Hz synchronous reluctance motors

When the motor is at a standstill, the background signal noise of the continuous shaft-flux-linkage signals for 1 second is shown in fig. 6. Since the motor is not running, there is no bouncing of the signal brushes. The noise is picked up electromagnetically from the environment. For comparison purposes the unit for magnitudes of shaft-flux-linkage signals remains the same throughout this study.

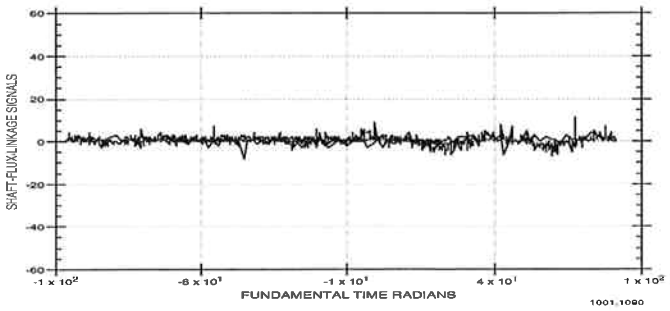

Fig. 6. Background signal noise of continuous shaft-flux-linkage signals of a 4-pole synchronous reluctance motor for 1.0 s at standstill

V. Tests On Synchronous Reluctance Machines For Relationships Between Eccentricities And Shaft Signals

No-load comparisons

Fig. 7 shows the superposed loci of continuous shaft-flux-linkage signals for individual revolutions of the synchronous reluctance motors. The thickness of the loci represents the variations that include the effects of the non-synchronized dynamic eccentricities. The overall signal magnitude reflects eccentricities and other relevant asymmetrical situations mentioned previously. The high-magnitude spikes are noises produced by bouncing signal brushes.

In order to compare the loci of continuous shaft-flux-linkage signals under different eccentricities among the three motor assemblies, the line voltages of 230 volts, the time duration of 1 second, and the decoupling condition of the motors from the generator remain practically identical as those for the loci of #1 motor shown in fig. 7a. The overall signal magnitude shown in 7a is 46 as compared with that of 37 for the #2 motor shown in fig. 7b. A low overall magnitude of 27 for the #3 motor is shown in fig. 7c. A snapshot of the locus for the #3 motor is illustrated in fig. 8. On the basis of these three tests, one may conclude that the air gap clearly affects the magnitudes of the shaft-flux-linkage signals. The loci have certain thicknesses that reflect the non-synchronized eccentricities along with other non-synchronized asymmetries.

One may choose to use different sweeping inputs for superposed loci of continuous shaft-flux-linkage signals. Fig. 9 shows the traces when a sine-wave voltage is used for the sweeping input by stepping down a phase voltage from the supply. Since $\sin(\pi/6) = 0.5$ and $\sin(\pi/2) = 1$, the horizontal scale is not linear. This approach ignores the positional char-

order harmonic is further modulated by a two-pole cosine term. It is also noted from the angular frequencies of (7) and (6) that if the electrical frequency for the main poles is 60 Hz (i.e., 60 Hz · 3/3), the frequency for the 8th mechanical order is 60 Hz · 8/3 =) 160 Hz, and for the fundamental (2-pole) mechanical order is (60 Hz · 1/3 =) 20 Hz. This prediction is clearly confirmed in the experiments. Without derivation here, it should be mentioned that other air-gap harmonics exist. These air-gap harmonic fluxes have their individual effectiveness to link with the shaft for shaft voltage generations.

III. Experimental Setups

The collection of shaft signals in this study is very primitive. It relies on two #10 stranded, VW-1 rated copper wires that ride on each end of the shaft. A 1 kΩ resistor as shown in fig. 2 is connected in parallel with the resistor-capacitor (RC) integrator for absorbing partial noise in the circuit. At 60 Hz the reactance of the capacitor is only 4 kΩ, the current of this RC circuit is dictated by the 33 kΩ resistor. Since the current in a resistor is directly proportional to the voltage, the voltage across the capacitor closely represents the integration of voltage. This integration results in a voltage proportional to the shaft flux linkages. Smaller capacitance produces higher magnitudes of integration signals but with greater errors from the capacitive current components. However, moderate errors may be acceptable in practice. The grounding of the frame uses the same wire that grounds the signal and the oscilloscope. Single grounding point prevents the potential differences from various grounding points that may cause noises. A dc-20MHz digital storage oscilloscope with a minimum scale of 2 mV/div. and a personal computer with data acquisition and plotting software packages are used.

Two different types of machines are used in the tests. One is the synchronous reluctance machine; the other type is the wound field synchronous machine.

The synchronous reluctance machines are modified from 4-pole, 5 Hp, 60 Hz, 230 V, parallel-Y, induction machines. Four, half-inch-deep grooves are milled on the rotor surface. The axial length of the grooves is the rotor core length and the width of each groove equals the pole width. End rings of the original squirrel cage are retained for starting purposes. The original air gap per side is 0.356 mm. Additionally, the rotor outside diameter is machined off 0.381 mm per side for the reluctance machine.

The reluctance machine can be coupled to a dc generator through a digital torque gauge and tachometer. The couplings are of insulated type. The half coupling on the reluctance motor shaft can be slid back after loosening its set screw when decoupling is required.

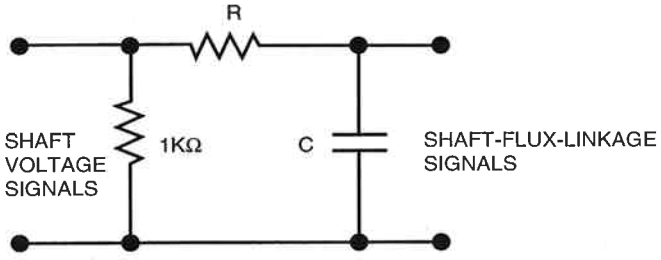

Fig. 2. A simple resistor-capacitor integrator (R = 33 kΩ, c = 0.66 μF)

The end bracket on the driving side of the reluctance machine is the original one without machining. The bearing housing of a non-driving-side end bracket is enlarged to accommodate two layers of 0.0508 mm thick kapton tapes. The flange of the same end bracket is machined off 0.737 mm per side. The value of 0.737 mm is derived from the sum of the original air gap (0.356 mm) and the additional air gap (0.381 mm). This end bracket is named the "modified end bracket" for identification purpose.

Four equally spaced holes are drilled, respectively, at each end bracket. Centers of these holes are lined up with the rotor diameter for air-gap measurements by feeler gauges. Unfortunately, this is proven to be rather difficult in practice for sticking a long and thin filler gauge to measure very small gaps in an extremely dim environment. Therefore, comparisons are made on the basis of three different assemblies of the non-driving side. The stator, rotor, and driving-side end bracket remain unchanged throughout comparisons. The differences in these three motor assemblies that only have changes in eccentricities are:

Motor #1: Original bearing with original end bracket of the non-driving side.

Motor #2: Bearing wrapped with two layers of tapes and located in bearing housing of the modified end bracket. The flange location is selected purely by feeling for a position where the rotor is not rubbing the stator. Axial through screws are tightened to secure the end brackets locations.

Motor #3: Bearing wrapped with one layer of tape and loosely situated in bearing housing of the modified end bracket. Again, the flange radial location is selected randomly.

From a statistic's standpoint, regardless how random the flange positions may be, the chance to have three identical eccentricities among these three motor assemblies is very slim. The comparisons in this study are conducted under a rigid condition that all situations are as identical as possible when only the motor assemblies (or eccentricities) are changed. Other stand-alone assemblies are used to explain general features without comparison purposes.

The wound field synchronous machine is an old and oversized 6-pole, 230 V, 60 Hz, 15 kVA motor. The rated field current is 4 amps at 125 volts. It is mainly used for shorted field coil tests in this study.

IV. Positional Characteristic Of Shaft Voltages

Fig. 3 shows a snapshot of shaft-flux-linkage signals of the 4-pole #1 synchronous reluctance motor. The effects of eccentricities synchronized with every single revolution are reflected in the magnitudes of shaft-flux-linkage signals. Timewise, one revolution of a 4-pole synchronous machine equals two cycles of fundamental frequency. It is noticed from the trace that within any two fundamental cycles the waveforms per half cycle (or per pole) are not the same. Therefore, the minimum time for the shaft-flux-linkage signals to repeat itself is the time for one revolution. The reason is that the rotor is not absolutely symmetrical from electrical, magnetical, and mechanical standpoints. The relationship between the forward fundamental rotating field and the rotor

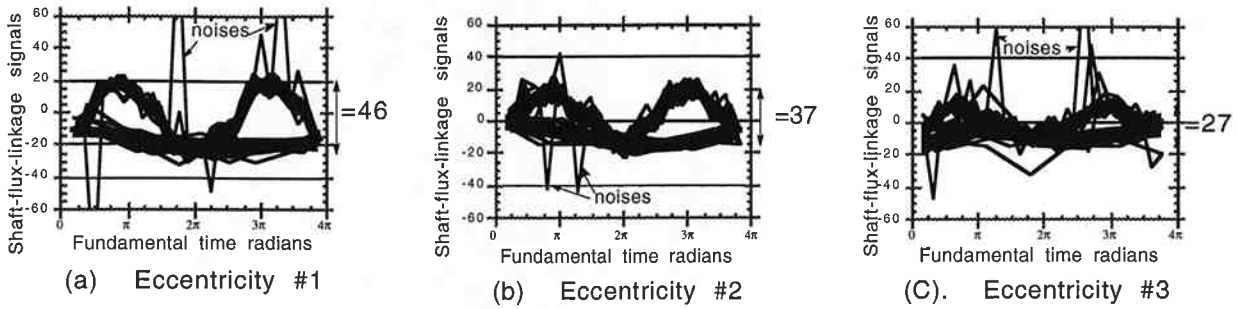

Fig. 7. Significant changes of overall shaft-flux-linkage-signal magnitudes under three different eccentricities of a 4-pole, synchronous reluctance motor. (Loci for continuous shaft-flux-linkage signals of 1.0 second are obtained at 60 Hz, 230 V, and no-load. Eccentricity is only controlled by changing end brackets and fits of bearings. All other parts of the motor remain unchanged).

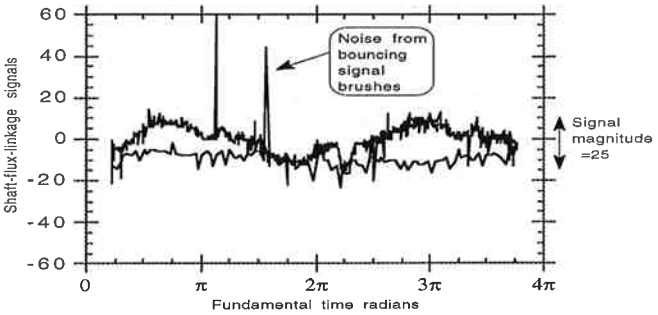

Fig. 8. Locus of shaft-flux-linkage signals and signal magnitude of 4-pole #3 synchronous reluctance motor for single sweep at 60 Hz, 230 V (phase currents: 11.3/11.1/11.1 A.)

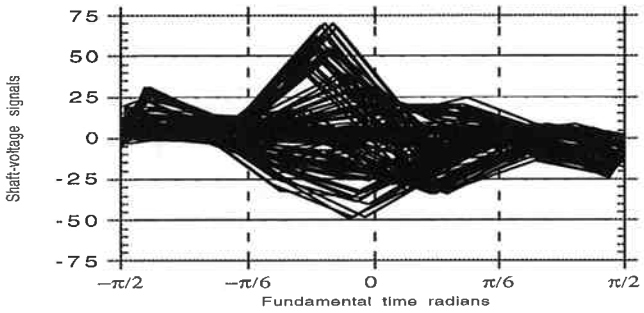

Fig. 9. Loci of shaft-voltage signals of reluctance motor #1 for 1 s at 60 Hz, 230 V, and 1,800 rpm under fundamental voltage for sweepings (phase currents: 11.1/10.5/10.7 A.)

acteristic of shaft signals and makes the loci clustery. The horizontal sweeping sine wave also creates difficulty in distinguishing the noise generated by the bouncing signal brushes.

Influence of fits between bearing and its housing

Motor assembly #3 has a loose fit between bearing and its housing at the non-driving end. When it is coupled to an unloaded dc generator through a torque gauge and tachometer, the air gap of the motor with a loose-fit bearing is significantly affected by the mechanical situation on the other side of the coupling. This is demonstrated by the great jump of the overall signal magnitude of 41 shown in fig. 10 from the 27 shown in fig. 7c. For the motor #2 with a tighter fit as shown in the following comparison, no such a great jump is encountered.

Influence of loads

Under an identical load of 8.5 Nm, the loci of motors #2 and #3 are shown in fig's 11 and 12 respectively. The overall signal magnitudes are 38 in both cases. While there is little change in the magnitude of #2 motor between the uncoupled no-load and the coupled and loaded situations (37 of fig. 7b versus 38 of fig. 11), there is a great jump for the #3 motor between the uncoupled and the coupled and loaded situations (27 of fig. 7c versus 38 of fig. 12). The difference between no-load and loaded situations of #3 motor is not very significant (41 of fig. 10 versus 38 of fig. 12).

VI. Tests Conducted On Wound-Field Synchronous Machines For Relationships Between Shorted Field Coil And Shaft Signals

Shaft voltages and shaft flux linkages

Fig. 13 shows the comparison of shaft voltages and shaft flux linkages at no load between situations with (fig. 13a) and without (fig. 13b) a shorted field coil of the wound-field synchronous motor. The field-coil short circuit is introduced by shorting one pole of the 6-pole field coils without permanent damage to the machine. The field excitation current is fed with a pure direct current without ripples. The upper traces in both (a) and (b) represent shaft voltages, and the lower traces are for shaft flux linkages. Further experiments indicate that the shaft-to-shaft signals are not significantly affected by the change of excitation source from a pure dc to a six-pulse full-wave rectifier.

The shaft flux linkage is obtained through an RC circuit depicted in fig. 2. Within the period for one mechanical revolution the shaft flux linkage shown in (a) has nine major cycles for the situation without shorted field coil. These nine cycles per one mechanical revolution correspond to the third-harmonic flux component. The shaft flux linkage shown in (b) has eight major cycles for the situation with a shorted field coil. The eight major cycles are further modulated by a variation of one cycle per revolution. This clearly confirms the theoretical predictions. For the situation with only few shorted turns instead of a shorted pole, the magnitude should be lower. However, the harmonic components can be traced accordingly.

Fig. 14 shows the comparison of the continuous loci of shaft flux linkage signals for one minute at no load between the situations with (fig. 14a) and without (fig. 14b) a shorted field coil of the same 6-pole synchronous motor. The nine

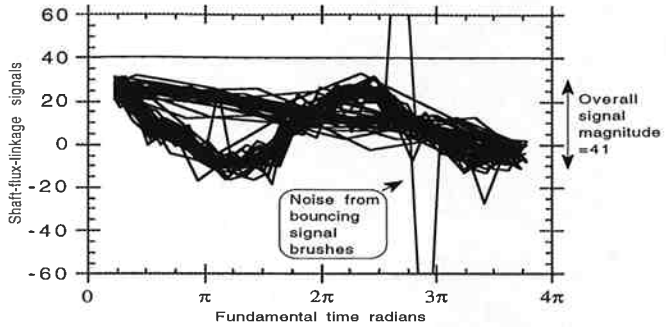

Fig. 10. Loci of shaft-flux-linkage signals and overall signal magnitude of 4-pole #3 synchronous reluctance motor coupled to generator for 1.0 s at 60 Hz, 230 V (phase currents: 11.5/10.9/10.9 A.)

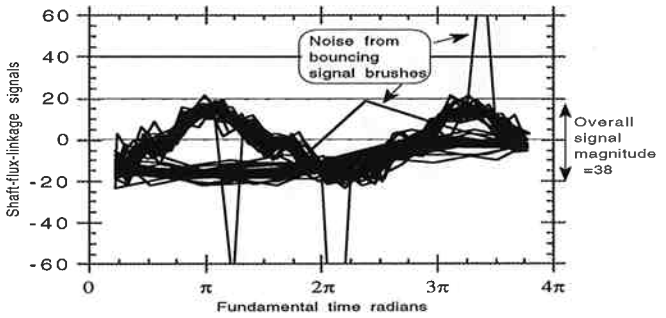

Fig. 11. Loci of shaft-flux-linkage signals and overall signal magnitude of 4-pole #2 synchronous reluctance motor under 8.5 Nm. load for 1.0 s at 60 Hz, 230 V (phase currents: 12.1/11.9/12.0 A.)

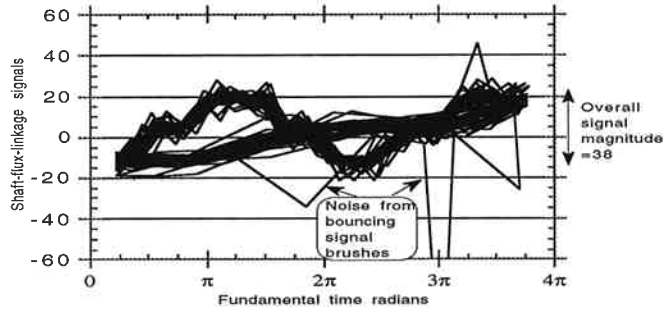

Fig. 12. Loci of shaft-flux-linkage signals and overall signal magnitude of 4-pole #3 synchronous reluctance motor under 8.5 Nm. load for 1.0 s at 60 Hz, 230 V (phase currents: 12.5/11.8/12.0 A.)

major peaks per one mechanical revolution of the situation without shorted field coil (fig.14a) are marked. Correspondingly, eight major peaks are also marked for the situation with a shorted field coil (fig. 14b).

Shaft flux linkage harmonics

The comparison of relative shaft-flux-linkage harmonics at no load between situations with and without a shorted field coil of the same 6-pole wound-field synchronous machine is shown in fig. 15. Two distinctive orders of harmonics around 20 Hz and 160 Hz as predicted are clearly shown in the situation with a shorted field coil (fig. 15b).

VII. Conclusions

Theoretically speaking, the greater the eccentricities are, the higher the shaft-flux linkages. There are specific harmonic components that are related to shorted field turns.

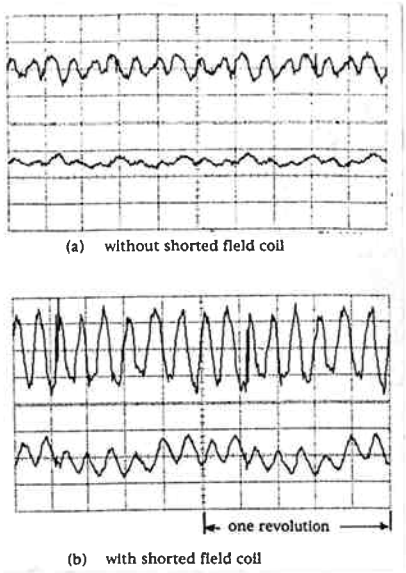

Fig. 13. Comparison of shaft voltages and shaft-flux linkages at no load between situations with and without shorted field coil of a 6-pole, wound-field synchronous motor excited by pure dc (1.4 and 1.6 amps). Stator line voltage is 230 V at 60 Hz
Upper traces: shaft-to shaft voltages, 70 mV/div.
Lowr traces: shaft-to-shaft flux linkages, 10 mV/div.
Horizontal scale: 10 ms/div.

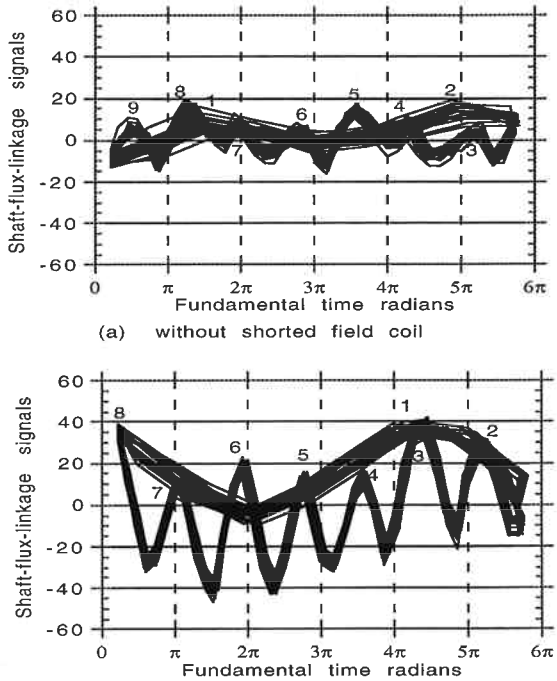

Fig. 14. Comparison of loci of shaft-flux-linkage signals for one second at no load between situations with and without shorted field coil of a 6-pole, synchronous motor excited by pure dc (1.4 and 1.6 amps). Stator line voltage is 230 V at 60 Hz

In order to record continuous loci of shaft signals, a ramp sweeping input that is synchronized with a given number of the line frequency cycles is used for the horizontal input of oscilloscope.

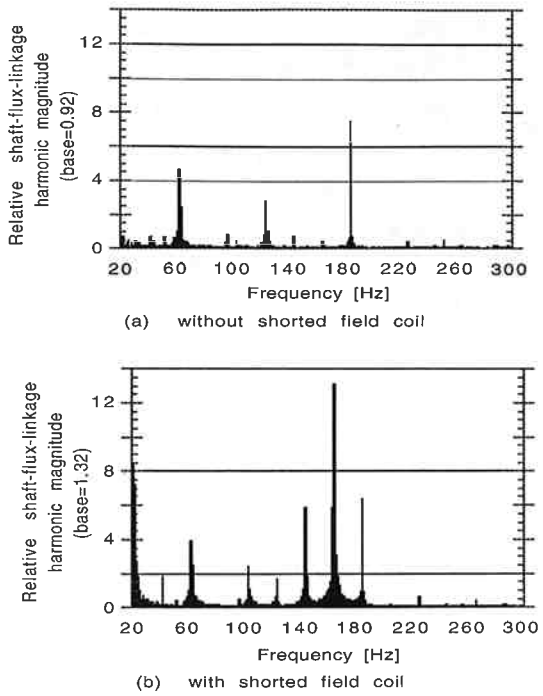

Fig. 15. Comparison of relative shaft-flux-linkage harmonic magnitudes at no load between situations with and without shorted field coil of a 6-pole, synchronous motor excited by pure dc (1.4 and 1.6 amps). Stator line voltage is 230 V at 60 Hz

Because of the positional characteristic, it is recommended that the minimum number of cycles for the ramp sweeping input is the number of cycles per revolution.

Eccentricity tests are conducted on three synchronous reluctance motor assemblies. All test conditions are kept as identical as possible except the eccentricities are different in the three motor assemblies.

The magnitudes and the thicknesses of shaft-signal loci reflect the synchronous and asynchronous steady and dynamic eccentricities with respect to the sweeping signals.

Significant changes in the loci magnitudes for the three different eccentricities are observed.

Eccentricities of loose-fit bearings are not stable. They vary according to what are coupled to their shafts.

There are little changes in magnitudes of shaft-flux-linkage signals from no-load to loaded situations of the experimental motors.

When a field coil is shorted, the 160 Hz and 20 Hz shaft-flux-linkage components of a 6-pole wound-field synchronous motor clearly confirm the validity of the theory.

Threshold loci records can be used for indications of changes in eccentricities and the defects of field coils.

VIII. Acknowledgments

The authors would like to thank the State of Texas for financial support under Texas Advanced Technology Program, Grant No. 1591 and 003658-181, through which the concepts were conceived. The authors are grateful for the partial financial support from the Electric Power Research Institute. Thanks are due to the Center for Electromechanics, The University of Texas at Austin, for the support staff and facilities provided for the research work. The typography was conducted by Ms. Mary Davis. Finally, the authors would like to express their appreciation to Dr. Herbert H. Woodson, Prof. William F. Weldon, and Mr. John H. Gully for their support and discussions in this research.

IX. References

[1] P. L. Alger and H. W. Samson, "Shaft Currents in Electric Machines," *Transactions AIEE*, February 1924, pp. 235-245.

[2] S. P. Verma and R. S. Girgis, "Shaft Potentials and Currents in Large Turbo Generators," Report for the Canadian Electrical Association, Research & Development, Suite 580, One Westmount Square, Montreal, Quebec, H3Z 2P9, May 1981.

[3] A. Meyer, R. Joho, Z. Posedel, K. Reichert, and C. Ammann, "Shaft Voltages in Turbosets: Recent Development of a New Grounding Design to Improve The Reliability of the Bearings," *International Conference on Large High Voltage Electric Systems*, 1988 Section, 28th August - 3rd September, Paris.

[4] C. Ammann, K. Reichert, and Z. Posedel, "Shaft Voltages in Turbosets: Operating Experience with RC-Grounding Device and New Possibilities for Monitoring the Condition of Turbogenerators," ibid.

[5] HYDROGENERATOR DESIGN MANUAL, Chapter 8, U.S. Department of Interior, Plant Equipment Section, Electrical Branch, Electrical and Mechanical Engineering Division, Bureau of Reclamation, Denver, Colorado, December, 1991.

[6] J. R. Cameron, W. T. Thomson, and A. B. Dow, "Vibration and Current Monitoring for Detecting Air Gap Eccentricity in Large Induction Motors," *IEEE Proceedings*, vol. 133, Pt. B, no. 3, May, 1986, pp. 155-163.

[7] A. J. Marques Cardoso, E. S. Saraiva, M. L. Sousa Mateus, and A. L. Ramalho, "On-Line detection of Air Gap Eccentricity in 3-phase Induction Motors by Park's Vector Approach," *Fifth International Conference on Electrical Machines and Drives, Conference Publication No. 341*, 11-13 September 1991, pp. 61-66.

[8] G. B. Pollock and J. F. Lyles, "Vertical Hydraulic Generators Experience with Dynamic Air Gap Monitoring," *IEEE Transactions on Energy Conversion*, vol. 7, no. 4, December 1992, pp. 660-667.

[9] M. J. DeBortoli, S. J. Salon, D. W. Burow, and C. J. Slavik, "Effects of Rotor Eccentricity and Parallel Windings on Induction Machine Behavior: A Study Using Finite Element Analysis," *Fifth IEEE Biennial Conference on Electromagnetic Field Computation*, Harvey Mudd College, Clearmont, California, August 3-5th, 1992.

[10] John S. C. Hsu (Htsui), Herbert H. Woodson, and Shy S. Liou, "Experimental Study of Harmonic Flux Effects in Ferromagnetic Materials," *IEEE Transactions on Magnetics*, vol. 25, pp. 2678-2685, May 1989.

John S. Hsu (or Htsui) was born in China. He received a BS degree from Tsing-Hua University, Beijing, China, and a Ph.D. degree from Bristol University, England, in 1959 and 1969, respectively. He joined the Electrical and Electronics Engineering Department of Bradford University, England, serving there for nearly two years.

After his arrival in the United States in 1971, he worked in research and development areas for Emerson Electric Company and later for Westinghouse Electric Corporation. He served as head of the Rotating Machines and Power Electronics Program, Center for Energy Studies, the University of Texas at Austin for over four years. Presently, he is a researcher at the Center for Electromechanics at The University of Texas at Austin.

Dr. Hsu is a chartered engineer in the United Kingdom and a registered professional engineer in Texas, Missouri, and New York.

Jan Stein received BS and MS degrees in electrical engineering from the Delft University of Technology in the Netherlands. Mr. Stein is with EPRI where he manages research projects related to power plant electrical systems and equipment. Mr. Stein is a member of the IEEE.